Pediatr Radiol (2017) 47:1809–1816
DOI 10.1007/s00247-017-3955-1

ORIGINAL ARTICLE

Long-term effects of radiation therapy on white matter of the corpus callosum: a diffusion tensor imaging study in children

Monwabisi Makola[1] · M. Douglas Ris[2] · E. Mark Mahone[3,4] · Keith Owen Yeates[5] · Kim M. Cecil[6,7,8,9,10]

Received: 20 March 2017 / Revised: 20 June 2017 / Accepted: 18 July 2017 / Published online: 26 August 2017
© Springer-Verlag GmbH Germany 2017

Abstract
Background Despite improving survival rates, children are at risk for long-term cognitive and behavioral difficulties following the diagnosis and treatment of a brain tumor. Surgery, chemotherapy and radiation therapy have all been shown to impact the developing brain, especially the white matter.
Objective The purpose of this study was to determine the long-term effects of radiation therapy on white matter integrity, as measured by diffusion tensor imaging, in pediatric brain tumor patients 2 years after the end of radiation treatment, while controlling for surgical interventions.
Materials and methods We evaluated diffusion tensor imaging performed at two time points: a baseline 3 to 12 months after surgery and a follow-up approximately 2 years later in pediatric brain tumor patients. A region of interest analysis was performed within three regions of the corpus callosum. Diffusion tensor metrics were determined for participants (n=22) who underwent surgical tumor resection and radiation therapy and demographically matched with participants (n=22) who received surgical tumor resection only.
Results Analysis revealed that 2 years after treatment, the radiation treated group exhibited significantly lower fractional anisotropy and significantly higher radial diffusivity within the body of the corpus callosum compared to the group that did not receive radiation.
Conclusion The findings indicate that pediatric brain tumor patients treated with radiation therapy may be at greater risk of experiencing long-term damage to the body of the corpus callosum than those treated with surgery alone.

Keywords Brain · Brain tumor · Children · Corpus callosum · Diffusion tensor imaging · Magnetic resonance imaging · Radiation · White matter

✉ Kim M. Cecil
kim.cecil@cchmc.org

[1] College of Medicine, University of Cincinnati, Cincinnati, OH, USA

[2] Department of Pediatrics, Baylor College of Medicine, Texas Children's Hospital, Houston, TX, USA

[3] Department of Neuropsychology, Kennedy Krieger Institute, Baltimore, MD, USA

[4] Department of Psychiatry & Behavioral Sciences, Johns Hopkins University School of Medicine, Baltimore, MD, USA

[5] Department of Psychology, Alberta Children's Hospital Research Institute, Hotchkiss Brain Institute, University of Calgary, Calgary, AB, Canada

[6] Imaging Research Center, Cincinnati Children's Hospital Medical Center, MLC 5033, 3333 Burnet Ave., Cincinnati, OH 45229, USA

[7] Department of Radiology, University of Cincinnati College of Medicine, Cincinnati, OH, USA

[8] Department of Pediatrics, University of Cincinnati College of Medicine, Cincinnati, OH, USA

[9] Neuroscience Graduate Program, University of Cincinnati College of Medicine, Cincinnati, OH, USA

[10] Department of Environmental Health, University of Cincinnati College of Medicine, Cincinnati, OH, USA

Introduction

The incidence of pediatric central nervous system (CNS) tumors has been on the rise during the last 40 years with 1.9 cases per 100,000 in 1973 [1] and 5.4 cases per 100,000 for children under 19 years by 2013 [2]. Survival rates for pediatric CNS tumor patients have also been on the rise, largely due to improved diagnostic techniques and therapeutic approaches. The 5-year survival rate for patients younger than 19 years at the time of primary brain tumor diagnosis was 66% from 2000 to 2004; however, by 2013, the rate increased to 73% [2].

Gross total tumor resection remains the gold standard of treatment. In many cases, however, complete tumor resection is not possible. Subsequently, the multipronged approach of surgery, chemotherapy and radiation therapy is commonly employed in the treatment of CNS tumors. Approximately 200,000 patients of all ages receive partial or whole brain radiation therapy to treat primary or metastatic brain tumors every year in the United States [3]. However, using radiation therapy to treat pediatric CNS tumors comes at some cost in terms of neurodevelopmental morbidity. Research shows that children treated with radiation therapy are susceptible to radiation-induced cognitive impairment, a condition characterized by poor behavioral, emotional and cognitive outcomes. Deficits in intelligence quotient (IQ), scholastic development, memory, attention and information processing speed have all been reported [4–9]. These sequelae have been found in children who received both diffuse and focal radiation therapy [7, 8, 10, 11]. Longitudinal studies show that children treated with radiation therapy for brain tumors exhibit an elevated risk for a poorer quality of life compared to their healthy siblings; they are less likely to be employed or to be able to engage in complex motor tasks, such as driving a car [8]. Survivors also have an increased risk of developing academic difficulties, with many requiring remedial classes in mainstream schools or placement in special-needs classrooms [7, 8, 10].

Radiation therapy can have a profound effect on the brain. Vascular damage, multifocal hemorrhage, edema, neuroinflammation, astrogliosis and neuronal cell damage are common findings [12, 13]. Cellular damage is not limited to neurons, but extends to glial cells, with oligodendrocytes being particularly vulnerable. Oligodendrocytes have high metabolic demands and mitochondrial content, making them sensitive to the oxidative stress caused by radiation [14, 15]. Damage to oligodendrocyte progenitor cells and fully differentiated oligodendrocytes with subsequent white matter necrosis due to axonal demyelination and degradation has been observed [3, 14, 16, 17].

Diffusion tensor imaging is a magnetic resonance imaging (MRI) technique useful for characterizing white matter integrity. Diffusion tensor imaging relies on the diffusion characteristics of water to depict white matter tracts in the brain. Without barriers, the random, Brownian movement of water molecules is isotropic or uniform in all directions. The presence of membranes, fibers, myelin and other such barriers creates anisotropic water diffusion, which is greater in one direction than others.

Diffusion tensor imaging studies have shown that radiation therapy has a negative effect on white matter integrity [18, 19] and that this radiation therapy-induced decline in white matter integrity is associated with poor cognitive outcomes [20]. However, many of these studies focused on white matter changes within the first year following the commencement of radiation therapy. Many patients who receive radiation therapy do so after undergoing surgical tumor resection and little work has been done to account for the possible effects of surgical intervention. The purpose of this study was to determine the long-term effect of radiation therapy on white matter integrity, as measured by diffusion tensor imaging, in pediatric brain tumor patients 2 years after the end of radiation treatment, while controlling for surgical interventions. This study evaluated the hypothesis that children treated with surgery and radiation therapy, with and without chemotherapy, will exhibit reduced white matter integrity compared to those treated with surgery only.

Materials and methods

Study participants

This study is part of a longitudinal project focused on cognitive, behavioral, socio-emotional and imaging outcomes following pediatric brain tumor treated with or without radiation. Participants included pediatric brain tumor patients recruited from neuro-oncology clinics at four different urban medical centers: Cincinnati Children's Hospital Medical Center in Cincinnati, Ohio; Dayton Children's Hospital in Dayton, Ohio; Nationwide Children's Hospital in Columbus, Ohio, and Kennedy Krieger Institute in Baltimore, Maryland (Table 1).

All procedures performed in studies involving human participants were in accordance with the ethical standards of the institutional and/or national research committee and with the 1964 Helsinki declaration and its later amendments or comparable ethical standards.

During recruitment, 271 patients who had recently undergone brain tumor resection were screened for inclusion in the study. Thirty patients were ruled out due to severe preexisting conditions or ineligible tumors, which included glioblastoma multiforme and intrinsic brain stem glioma. Patients with these tumors were excluded because their poor prognosis is not ideal for inclusion in a longitudinal study. An additional 93 patients were excluded due to severe postsurgical complications and 35 patients were excluded due to a history of neurofibromatosis type 1, a genetic disorder associated with functional and cognitive difficulties outside the occurrence of tumors. Of the 113 eligible potential participants, 44 declined to participate and the remaining 69 were enrolled into the study. Informed assent and

Table 1 Group demographic and tumor-related variables

Variable	Baseline		2-year	
	No-RT (*n*=22)	RT (*n*=22)	No-RT (*n*=14)	RT (*n*=14)
Gender (male/female)	15/7	19/3	11/3	12/2
Age at baseline (y) (m [SD])	10.14 (4.39)	9.68 (3.77)	10.07 (4.32)	10.07 (4.03)
Location				
Cincinnati	16	15	11	8
Dayton	-	1	-	1
Columbus	4	4	1	3
Baltimore	2	2	2	2
Scanner				
GE Signa 1.5 Tesla	15	15	11	11
GE Signa 3 Tesla	2	2	2	2
Siemens 3 Tesla	5	5	1	1
Tumor type				
Glioma	18[a]	3	13	1
ATRT	-	1	-	1
Choroid plexus papilloma	1	1	-	1
Craniopharyngioma	1	1	-	-
Ependymoma		2	-	1
Germ cell	-	3	-	3
Dysembryoplastic neuroepithelial Tumor	1	-	1	-
Medulloblastoma/PNET	-	11	-	7
Meningioma	1	-	-	-
Tumor location				
Infratentorial	8	14	7	7
Supratentorial	14	8	7	7
Primary lesion size (mm^3) (m [SD])	1286.52 (1302.40)	1300.78 (870.6)	1692.38 (1443.21)	1343.87 (886.29)
Chemotherapy	Total 1	Total 16	-	Total 10
Platinum based	1	13	-	9
Vincristine	1	13	-	9
Type of radiation				
CR	-	1	-	1
CSRT	-	12	-	9
Focal	-	8	-	4
Total radiation (Gy) (m [SD])	-	53.19 (4.43)	-	52.75 (4.55)

ATRT atypical teratoid rhabdoid tumor, *CR* cranial radiation therapy, *CSRT* craniospinal radiation therapy, *Gy* gray, *m* arithmetic mean, mm^3 cubic millimeter, *No-RT* no radiation therapy group, *PNET* primitive neuroectodermal tumor, *RT* radiation therapy group, *SD* standard deviation, *y* years

[a] Within the No-RT group, all astrocytomas were classified as low grade with the majority as pilocytic astrocytomas

parental consent were obtained for all individual participants. Participants were separated into two groups based on tumor treatment. The radiation therapy group (RT) included participants who underwent surgical tumor resection and adjuvant radiation therapy, with or without chemotherapy. The comparison group was comprised of participants who received surgical tumor resection and no radiation therapy (No-RT). Members of the No-RT group were matched to members of the RT group based on age and MRI scanner type, evaluated at a postsurgical baseline and a 2-year follow-up time point. Table 2 reconciles participant enrollment numbers with participant imaging numbers included in this analysis.

Image acquisition

Imaging was conducted from August 2005 to August 2011 on three types of MRI scanners: a Trio 3-Tesla scanner (Siemens Medical Solutions, Malvern, PA, USA), a Signa 1.5-Tesla scanner (General Electric Healthcare, Chicago, IL, USA), and a Signa 3-Tesla scanner (General Electric Healthcare,

Table 2 Loss from enrollment: available imaging for analyses

Time point	Group	Initial	Deceased	Dropout	Lost to follow-up	Technical malfunction	Unable to match demographic variables [a]	Total
Baseline	No-RT	39	1	4	1	3	8	22
	RT	30	1	2	3	1	1	22
2 years	No-RT	30	0	3	4	0	9	14
	RT	23	3	1	4	0	1	14

No-RT No-radiation therapy group, *RT* radiation therapy group

[a] Members of the No-RT group were matched to members of the RT group based on age and scanner type

Chicago, IL, USA). Diffusion tensor imaging data from two examinations were evaluated. Baseline imaging was conducted 3–12 months after surgery and follow-up imaging was acquired 2 years (+/−3 months) after baseline. The baseline time point was selected to ensure the resolution of any acute neurosurgical effects, such as edema, for all participants, while preceding the onset of any delayed late effects of radiation therapy in the RT group. The diffusion tensor imaging protocols for the participants in the study are listed in Table 3.

Image processing

Variations in tumor location and surgical resection cavities made atlas-based image processing impractical as the transformations created severe image distortions for some participants. This analysis employed a region of interest (ROI)-based approach with three ROIs constructed to extract diffusion tensor imaging metrics. They included the genu, body and splenium of the corpus callosum. With our limited sample size, these three regions were chosen because of the strong association with cognitive performance and the technical factors associated with defining white matter tracts. Data were analyzed using DTI Studio and ROI Editor software packages (Laboratory of Anatomical Brain MRI, Johns Hopkins University, Baltimore, MD) [21]. Images were checked for artifacts; slices exhibiting severe distortions were excluded. To maximize the integrity of the diffusion tensor maps, image masks were created to minimize distortion from the background noise of the scans. Also, due to the small sample size, we limited our tensor calculation to three diffusion metrics: fractional anisotropy (FA), axial diffusivity and radial diffusivity. The diffusion maps were saved in the "Analyze" format in DTI Studio and reopened in ROI Editor for ROI drawing. For each diffusion tensor imaging data set, the diffusion maps were simultaneously imported into ROI Editor and ROIs were manually drawn onto the axial plane of the FA map (Fig. 1). A minimum FA threshold of 0.2 was set for each voxel before the acquisition of ROI values to ensure that only areas of white matter were recorded in each ROI. Any voxels falling below this threshold in the FA map were excluded from all three diffusion maps when the ROI values were calculated.

Statistical analysis

The three diffusion metrics for each participant ROI were imported into SigmaPlot (Systat Software, Inc., San Jose, CA) [22] for statistical analysis. Student's *t*-tests were used to compare the change in diffusion metrics between the No-RT group and the RT group at the two time points. Paired *t*-tests were used to compare within the two groups over time. Cohen's d value and effect size correlations were determined using group mean and pooled standard deviation values.

Results

Analysis of the postsurgical baseline data did not reveal any statistically significant differences in diffusion metrics for the genu, splenium and body of the corpus callosum between the No-RT and the RT groups (Table 4). For the majority of the RT participants, baseline imaging occurred 1–6 months after completing radiation therapy (median:

Table 3 Diffusion tensor imaging acquisition parameters

Scanner	Sequence	TR (ms)	TE (ms)	Voxel size (cm)	Directions
GE Signa 1.5 T	2-D SE EPI	12,000	81	3x3x3	15
GE Signa 3 T	2-D SE EPI	6000	71–87	3x3x3	25
Siemens TRIO 3 T	2-D SE EPI	6000	87	2x2x2	12

cm centimeter, *GE* General Electric, *ms* milliseconds, *T* Tesla, *TE* echo time, *TR* repetition time, *2-D SE EPI* 2-dimensional, spin echo, echo planar imaging

b values for all scanners: 0 and 1000 s/mm^2

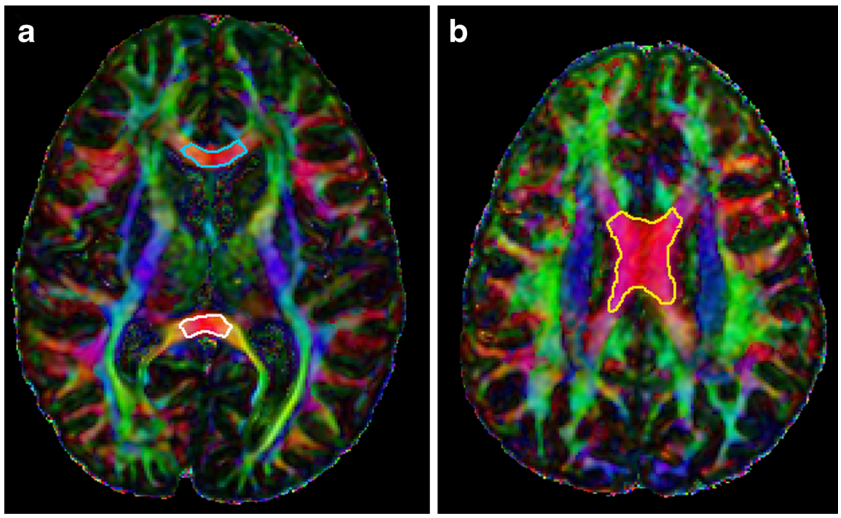

Fig. 1 Fractional anisotropy maps shown within the axial plane illustrate the regions of interest drawn in the study. **a** The genu, traced in *blue*, and the splenium, traced in *white*, of the corpus callosum. **b** The tracing, shown in *yellow*, illustrates the body of the corpus callosum. Color coding for fiber directions: *red*, right to left; *blue*, inferior to superior; *green*, anterior to posterior

1.2 months). At the 2-year time point, the RT group exhibited significantly lower FA and significantly higher radial diffusivity in the body of the corpus callosum compared to the No-RT group (Table 4). Conversely, no significant group differences in FA or radial diffusivity were observed in the genu or splenium of the corpus callosum, and no significant group differences were observed for axial diffusivity within any of the 3 ROIs at the postsurgical baseline or 2-year time point (not shown). To assess within group changes over time, we restricted our analysis to the body of the corpus callosum. Fourteen participants in each group, with both imaging studies performed on the same scanner type, were compared. Within the RT group, FA of the body of the corpus callosum exhibited significantly lower values and radial diffusivity exhibited significantly higher values at the 2-year time point compared to that from postsurgical baseline (Table 5).

Discussion

Pediatric brain tumor patients treated with radiation therapy, with or without chemotherapy, exhibited significantly reduced white matter integrity of the body of the corpus callosum compared to those treated without radiation therapy more than 2 years after the end of their treatment, while no such differences were observed between the two groups of patients within the first 3–12 months following treatment. This pattern of findings suggests that radiation therapy may confer greater long-term damage to white matter than surgery alone.

FA increases with CNS maturation because increasing axonal structure, membrane integrity and myelination creates a preferred diffusion direction [23]. Damage to axonal structures, membranes and myelination reduces the coherence of the preferred main diffusion direction, thus decreasing FA. Axial diffusivity is sensitive to changes in the diffusion of

Table 4 Comparison of corpus callosum diffusion metrics between groups at each time point by location

Diffusion metric	Postsurgical baseline (*n*=44)								2-year follow-up imaging (*n*=28)							
	RT			No-RT					RT			No RT				
	n	mean	SD	*n*	mean	SD	*P*	d	*n*	mean	SD	*n*	mean	SD	*P*	d
FA body	22	0.69	0.11	22	0.69	0.099	0.83	−0.069	14	0.61	0.091	14	0.71	0.081	**0.005**	−1.16
FA genu	22	0.80	0.070	22	0.79	0.058	0.60	0.16	14	0.77	0.047	14	0.80	0.045	0.17	−0.52
FA splenium	22	0.76	0.079	22	0.75	0.097	0.62	0.16	14	0.77	0.075	14	0.76	0.066	0.87	0.057
RD body	22	0.00068	0.00026	22	0.00063	0.00024	0.48	0.21	14	0.00089	0.00024	14	0.00062	0.00026	**0.017**	0.97
RD genu	22	0.00046	0.00019	22	0.00048	0.00017	0.75	−0.010	14	0.00052	0.00010	14	0.00048	0.00013	0.43	0.32
RD splenium	22	0.00054	0.00022	22	0.00057	0.00034	0.72	−0.11	14	0.00051	0.00020	14	0.00052	0.00017	0.89	−0.054

Student's *t*-tests were used to compare the change in diffusion metric (FA or RD) for a given ROI (genu, splenium or body of the corpus callosum) *between* the RT and No-RT groups at each time point (postsurgical baseline and 2-year follow-up imaging). Participant groups were matched based upon age and MRI scanner type

d Cohen's effect size, *FA* fractional anisotropy, *n* number of participants within the group, *No-RT* no radiation therapy group, *P* statistical significance *p*-value (<0.05 considered statistically significant and noted in bold), *RD* radial diffusivity, *RT* radiation therapy group, *SD* standard deviation

Table 5 Comparison of diffusion metrics for the body of the corpus callosum within groups over time

Diffusion metric	No-RT (*n*=28)								RT (*n*=28)							
	Postsurgical baseline			2-year follow-up					Postsurgical baseline			2-year follow-up				
	n	mean	SD	*n*	mean	SD	*P*	d	*n*	mean	SD	*n*	mean	SD	*P*	d
FA BCC	14	0.64	0.11	14	0.66	0.11	0.58	0.16	14	0.70	0.11	14	0.63	0.11	**0.012**	−0.62
RD BCC	14	0.00069	0.00027	14	0.00073	0.00035	0.64	0.13	14	0.00066	0.00028	14	0.00084	0.00028	**0.027**	0.64

Paired ***t***-tests were used to compare the change in diffusion metric (FA or RD) for the body of the corpus callosum *within* the RT and No-RT groups over time

BCC body of the corpus callosum, *d* Cohen's effect size, *FA* fractional anisotropy, *n* number of participants within the group, *No-RT* no radiation group, *P* statistical significance *p*-value (<0.05 considered statistically significant and noted in bold), *RD* radial diffusivity, *RT* radiation therapy group, *SD* standard deviation

water parallel to the long axis of white matter tracts [23–26] and reflects changes in axonal integrity. Radial diffusivity is best suited for measuring the degree of axonal myelination because it provides information about the diffusion characteristics of water perpendicular to the long axis of white matter tracts [27–29]. Strong evidence indicates that increases in radial diffusivity are indicative of white matter demyelination; as the amount or quality of the myelin around an axon decreases, it becomes easier for water to diffuse through the walls of the axon, causing an increase in radial diffusivity.

Decreases in FA [18, 19, 30–32] and increases in axial diffusivity and radial diffusivity [18, 33] have been observed in brain tumor patients treated with radiation. Unfortunately, the literature is sparse when it comes to the effects of surgery and chemotherapy on white matter integrity. One study found that pediatric brain tumor patients treated with surgery alone and those treated with surgery, chemotherapy and radiation therapy both experienced reductions in the FA of the body of the corpus callosum after treatment, but these reductions were only significant in the radiation therapy patients [19]. Similar to the current study, the surgery-only patients were diagnosed with pilocytic astrocytomas while those receiving surgery, chemotherapy and radiation therapy had medulloblastomas.

A potential confounder in the current study is tumor location. At the postsurgical baseline time point, there is a mismatch of infratentorial and supratentorial tumors. The surgical effects upon the corpus callosum of a supratentorial primitive neuroectodermal tumor (PNET) differ from those of a posterior fossa medulloblastoma. For both, the baseline and 2-year time points of the current study, the radiation therapy group included one patient with a supratentorial PNET. The more severe disease course or the addition of chemotherapy also may have affected the white matter integrity. Pediatric brain tumor patients receiving chemotherapy consisting of, but not limited to, vincristine and carboplatin without surgery or radiation therapy have been observed to experience significant decreases in the FA of the corpus callosum [34]. The possibility that chemotherapy affected the white matter integrity of the RT group cannot be ruled out by our study.

As the largest neural fiber bundle in the human brain with more than 200 million nerve fibers connecting the left and right cerebral hemispheres, the corpus callosum plays an indispensable role in our ability to coordinate movements, communicate and engage in critical thinking. The white matter integrity of the corpus callosum, as measured by diffusion tensor imaging, is positively related to information processing speed [35–38], which in turn mediates reasoning ability [39].

Group variability with respect to scanner usage, tumor location and treatment course, specifically, chemotherapeutic regimes, are key limitations that ultimately resulted in the primary limitation of this study, the small sample size. The study sites consisted of multiple centers designed to support enrollment for the broader neurobehavioral aims. Our overall study design allowed for recruitment of a RT group participant at one site and a No-RT participant at another site. Unfortunately, not every location used scanners with the same vendor or the same magnetic field strength. To minimize the research burden on participants, the research imaging was usually added on to the routine clinical imaging examination. Also, one site had the initial study-designated MRI scanner replaced during the course of the study. Diffusion tensor imaging sequence parameters, such as field strength, have a significant effect on the signal to noise ratio and the determined diffusion metrics. To account for technical differences in the parameters, each comparison group matched numbers of participants with diffusion tensor imaging data acquired on a particular scanner type.

Although significant changes have been observed in the genu and splenium of the corpus callosum in similar studies [18, 20], such findings did not occur in this study. The effects of age and dose could explain our lack of findings in genu and splenium. Nagesh et al. [18] found in the genu and splenium of the corpus callosum in adults (median: 60 years, range: 23

to 75 years), treated with biologically corrected doses of 50–81 Gy, a linear, dose-dependent increase in radial diffusivity and axial diffusivity starting at 3 weeks and continuing to 32 weeks from the start of radiation therapy. With the current study, the age at baseline is lower (median: 10 years, range: 3 to 16 years) and the total radiation dose is within a smaller range (median: 54 Gy, range: 45–59.4 Gy). A lack of statistical power could also be magnified by the partial volume effect. Partial volume effect reflects intra-voxel heterogeneity arising from different structures [40–42] and impacts diffusion tensor imaging values for the ROIs [43]. The values of larger fiber tracts are inherently more accurate than those of smaller tracts because they are averaged from a larger number of voxels. The partial volume effect causes voxels on the periphery of ROIs, which are in close proximity to structures of differing diffusion characteristics, to be "contaminated" by the values of their neighbors.

Increased intracranial pressure, ventriculomegaly, hydrocephalus and treatment with shunting could also impact the white matter integrity [44–46]. However, our groups were balanced to minimize potential effects. At baseline, each group had a nearly equivalent number of patients with and without hydrocephalus and with shunts (one per group). Post surgery, three patients had a shunt inserted, one in the radiation group, two in the surgery only group. However, the shunts did not cause artifact within the ROIs for the current study.

The imaging examinations were carried out for the majority of participants on 1.5-Tesla scanners. This limited the visualization of other white matter tracts and the ability to perform tensor calculations on crossing white matter fibers. The corpus callosum was among the easiest tracts to visualize and reproducibly draw ROIs within, as these structures are myelinated early in development and were tumor free in our study population.

A baseline time point of 3–12 months after surgery was chosen to allow for the resolution of postsurgical volume changes and edema. This may have come at some expense in terms of accounting for white matter damage as it has been shown that surgery alone can cause significant decreases in the FA of the rostral body of the corpus callosum before the commencement of radiation therapy in pediatric brain tumor patients. Once these patients undergo radiation therapy, those with a surgically affected body of the corpus callosum exhibit a significantly greater reduction in FA than those without a surgically affected body of the corpus callosum [32].

Conclusion

The findings from this study suggest that pediatric brain tumor patients treated with radiation therapy may be at greater risk of experiencing long-term damage to the body of the corpus callosum than those treated without radiation therapy. This damage may occur through axonal demyelination.

Acknowledgements Funding to support this work came from the National Institutes of Health grant numbers R01 CA112182, R01 ES027724 and the Intellectual & Development Disabilities Research Center, at Kennedy Krieger Institute, grant number U54 HD079123.

Compliance with ethical standards

Conflicts of interest None

References

1. Patel S, Bhatnagar A, Wear C et al (2014) Are pediatric brain tumors on the rise in the USA? Significant incidence and survival findings from the SEER database analysis. Childs Nerv Syst 30: 147–154
2. Ostrom QT, Gittleman H, Fulop J et al (2015) CBTRUS statistical report: primary brain and central nervous system tumors diagnosed in the united states in 2008-2012. Neuro Oncol 17(Suppl 4):iv1-iv62
3. Greene-Schloesser D, Moore E, Robbins ME (2013) Molecular pathways: radiation-induced cognitive impairment. Clin Cancer Res 19:2294–2300
4. Conklin HM, Ashford JM, Di Pinto M et al (2013) Computerized assessment of cognitive late effects among adolescent brain tumor survivors. J Neuro-Oncol 113:333–340
5. Lee YW, Cho HJ, Lee WH, Sonntag WE (2012) Whole brain radiation-induced cognitive impairment: pathophysiological mechanisms and therapeutic targets. Biomol Ther 20:357–370
6. Palmer SL, Armstrong C, Onar-Thomas A et al (2013) Processing speed, attention, and working memory after treatment for medulloblastoma: an international, prospective, and longitudinal study. J Clin Oncol 31:3494–3500
7. Mulhern RK, Palmer SL, Reddick WE et al (2001) Risks of young age for selected neurocognitive deficits in medulloblastoma are associated with white matter loss. J Clin Oncol 19:472–479
8. Mulhern RK, Merchant TE, Gajjar A et al (2004) Late neurocognitive sequelae in survivors of brain tumours in childhood. Lancet Oncol 5:399–408
9. Dietrich J, Monje M, Wefel J, Meyers C (2008) Clinical patterns and biological correlates of cognitive dysfunction associated with cancer therapy. Oncologist 13:1285–1295
10. Mulhern RK, Palmer SL, Merchant TE et al (2005) Neurocognitive consequences of risk-adapted therapy for childhood medulloblastoma. J Clin Oncol 23:5511–5519
11. Ris MD, Packer R, Goldwein J et al (2001) Intellectual outcome after reduced-dose radiation therapy plus adjuvant chemotherapy for medulloblastoma: a Children's cancer group study. J Clin Oncol 19:3470–3476
12. Price RE, Langford LA, Jackson EF et al (2001) Radiation-induced morphologic changes in the rhesus monkey (Macaca Mulatta) brain. J Med Primatol 30:81–87
13. Vogel FS, Hoak CG, Sloper JC, Haymaker W (1958) The induction of acute morphological changes in the central nervous system and pituitary body of macaque monkeys by cobalt60 (gamma) radiation. J Neuropathol Exp Neurol 17:138–150
14. Burns TC, Awad AJ, Li MD, Grant GA (2016) Radiation-induced brain injury: low-hanging fruit for neuroregeneration. Neurosurg Focus 40:E3
15. Ishii A, Dutta R, Wark GM et al (2009) Human myelin proteome and comparative analysis with mouse myelin. Proc Natl Acad Sci U S A 106:14605–14610

16. Panagiotakos G, Alshamy G, Chan B et al (2007) Long-term impact of radiation on the stem cell and oligodendrocyte precursors in the brain. PLoS One 2:e588
17. Schultheiss TE, Stephens LC (1992) The pathogenesis of radiation myelopathy: widening the circle. Int J Radiat Oncol Biol Phys 23: 1089–1091 discussion 1093-1084
18. Nagesh V, Tsien CI, Chenevert TL et al (2008) Radiation-induced changes in normal-appearing white matter in patients with cerebral tumors: a diffusion tensor imaging study. Int J Radiat Oncol Biol Phys 70:1002–1010
19. Rueckriegel SM, Driever PH, Blankenburg F et al (2010) Differences in supratentorial damage of white matter in pediatric survivors of posterior fossa tumors with and without adjuvant treatment as detected by magnetic resonance diffusion tensor imaging. Int J Radiat Oncol Biol Phys 76:859–866
20. Chapman CH, Nagesh V, Sundgren PC et al (2012) Diffusion tensor imaging of normal-appearing white matter as biomarker for radiation-induced late delayed cognitive decline. Int J Radiat Oncol Biol Phys 82:2033–2040
21. Jiang H, van Zijl PC, Kim J et al (2006) DTIStudio: resource program for diffusion tensor computation and fiber bundle tracking. Comput Methods Prog Biomed 81:106–116
22. Systat Software I (2014) SigmaPlot for windows. Systat Software, Inc., San Jose
23. Soares JM, Marques P, Alves V, Sousa N (2013) A hitchhiker's guide to diffusion tensor imaging. Front Neurosci 7:31
24. Wozniak JR, Krach L, Ward E et al (2007) Neurocognitive and neuroimaging correlates of pediatric traumatic brain injury: a diffusion tensor imaging (DTI) study. Arch Clin Neuropsych 22:555–568
25. Le Bihan D, Mangin JF, Poupon C et al (2001) Diffusion tensor imaging: concepts and applications. J Magn Reson Imaging 13: 534–546
26. Basser PJ, Pierpaoli C (1996) Microstructural and physiological features of tissues elucidated by quantitative-diffusion-tensor MRI. J Magn Reson B 111:209–219
27. Basser PJ (1995) Inferring microstructural features and the physiological state of tissues from diffusion-weighted images. NMR Biomed 8:333–344
28. Basser PJ, Pajevic S, Pierpaoli C et al (2000) In vivo fiber tractography using DT-MRI data. Magn Reson Med 44:625–632
29. Xue R, van Zijl PC, Crain BJ et al (1999) In vivo three-dimensional reconstruction of rat brain axonal projections by diffusion tensor imaging. Magn Reson Med 42:1123–1127
30. Qiu D, Kwong DLW, Chan GCF et al (2007) Diffusion tensor magnetic resonance imaging finding of discrepant fractional anisotropy between the frontal and parietal lobes after whole-brain irradiation in childhood medulloblastoma survivors: reflection of regional white matter radiosensitivity? Int J Radiat Oncol Biol Phys 69:846–851
31. Khong PL, Kwong DLW, Chan GCF et al (2003) Diffusion-tensor imaging for the detection and quantification of treatment-induced white matter injury in children with medulloblastoma: a pilot study. AJNR Am J Neuroradiol 24:734–740
32. Uh J, Merchant TE, Li Y et al (2015) Effects of surgery and proton therapy on cerebral white matter of craniopharyngioma patients. Int J Radiat Oncol Biol Phys 93:64–71
33. Hope TR, Vardal J, Bjornerud A et al (2015) Serial diffusion tensor imaging for early detection of radiation-induced injuries to normal-appearing white matter in high-grade glioma patients. J Magn Reson Imaging 41:414–423
34. de Blank PM, Berman JI, Fisher MJ (2016) Systemic chemotherapy and white matter integrity in tracts associated with cognition among children with neurofibromatosis type 1. Pediatr Blood Cancer 63: 818–824
35. Borghesani PR, Madhyastha TM, Aylward EH et al (2013) The association between higher order abilities, processing speed, and age are variably mediated by white matter integrity during typical aging. Neuropsychologia 51:1435–1444
36. Genova HM, DeLuca J, Chiaravalloti N, Wylie G (2013) The relationship between executive functioning, processing speed, and white matter integrity in multiple sclerosis. J Clin Exp Neuropsychol 35:631–641
37. Kerchner GA, Racine CA, Hale S et al (2012) Cognitive processing speed in older adults: relationship with white matter integrity. PLoS One 7:e50425
38. Kourtidou P, McCauley SR, Bigler ED et al (2013) Centrum semiovale and corpus callosum integrity in relation to information processing speed in patients with severe traumatic brain injury. J Head Trauma Rehabil 28:433–441
39. Ferrer E, Whitaker KJ, Steele JS et al (2013) White matter maturation supports the development of reasoning ability through its influence on processing speed. Dev Sci 16:941–951
40. Alexander AL, Hasan KM, Lazar M et al (2001) Analysis of partial volume effects in diffusion-tensor MRI. Magn Reson Med 45:770–780
41. Frank LR (2001) Anisotropy in high angular resolution diffusion-weighted MRI. Magn Reson Med 45:935–939
42. Oouchi H, Yamada K, Sakai K et al (2007) Diffusion anisotropy measurement of brain white matter is affected by voxel size: underestimation occurs in areas with crossing fibers. AJNR Am J Neuroradiol 28:1102–1106
43. Pfefferbaum A, Sullivan EV (2003) Increased brain white matter diffusivity in normal adult aging: relationship to anisotropy and partial voluming. Magn Reson Med 49:953–961
44. Yuan W, Mangano FT, Air EL et al (2009) Anisotropic diffusion properties in infants with hydrocephalus: a diffusion tensor imaging study. AJNR Am J Neuroradiol 30:1792–1798
45. Patel SK, Yuan W, Mangano FT (2017) Advanced neuroimaging techniques in pediatric hydrocephalus. Pediatr Neurosurg. doi:10.1159/000454717
46. Siasios I, Kapsalaki EZ, Fountas KN et al (2016) The role of diffusion tensor imaging and fractional anisotropy in the evaluation of patients with idiopathic normal pressure hydrocephalus: a literature review. Neurosurg Focus 41:E12